International Journal of GEOMATE, May, 2020, Vol.18, Issue 69, pp. 9 - 17
ISSN: 2186-2982 (P), 2186-2990 (O), Japan, DOI: https://doi.org/10.21660/2020.69.5534
Geotechnique, Construction Materials and Environment

METHODOLOGY FOR MONITORING THE FLEXURAL BEHAVIOR OF STRUCTURAL CONCRETE MEMBERS WITH UNBONDED INTERNAL STEEL

Iqbal Peera[1] and * Nazar Oukaili[2]

[1], University of Baghdad, Iraq; [2], University of Baghdad, Iraq

*Corresponding Author, Received: 14 April 2019, Revised: 05 Dec. 2019, Accepted: 31 Jan. 2020

ABSTRACT: This paper presents a numerical methodology for a nonlinear analysis model to investigate the complete load vector versus strain vector and the deformational response of structural concrete members reinforced with unbonded post-tensioned steel and conventional nonprestressed steel. The adopted calculation procedure of this methodology includes an iterative algorithm for determining the strain and the stress in concrete, unbonded prestressed steel and nonprestressed steel at different loading steps including the ultimate stage. Based on the nonlinear analysis that performed at different sections along the beam and depending on the attained stress-strain state of the structural concrete member under the applied loading, the stress in unbonded steel is determined using an extensive iterative procedure. During any loading step, the analysis is repeated until the strains in concrete, unbonded prestressed steel, and nonprestressed steel are evaluated within a reasonable tolerance, an experimental verification was carried out using test results taken from four different investigations that performed between 1976 and 1991 on different flexural concrete members. It was observed that an excellent correlation was found between the results of the proposed methodology and the experimental tests.

Keywords: Internal unbonded tendon, Post-tensioning, Flexural stress, Constitutive relationship, Stiffness matrix

1. INTRODUCTION

The analysis of concrete members prestressed with unbonded steel is varying from that of concrete members prestressed with bonded steel. In the latter, the change in strain and thereby the change in stress beyond the effective prestress can be determined from strain compatibility between the bonded steel and adjacent concrete, so, it is a section dependent analysis. This procedure is not reliable for the concrete members prestressed with unbonded steel due to the lack of bonding between the post-tensioned steel and the surrounding concrete. The change in strain in the unbonded steel is a member dependent that is a function to the average change in the strain distribution along the adjacent concrete fibers over the whole length of the steel, so it can be assumed uniform between the anchorage zones of the member.

Several equations have been suggested for predicting the flexural stress at ultimate f_{ub} in unbonded prestressed steel based on the experimental studies carried out by different researchers depending on several variables as Warwaruk et al. [1], Pannell [2], Mattock et al. [3], and Mojtahedi and Gamble [4]. Based on these studies, different expressions were proposed for the flexural stress at ultimate f_{ub} and consequently to the methodologies adopted in international practice codes.

Over the last few years, researches with experimental and/or analytical studies have continued to be published to cover this important subject [5-15].

The ACI 318M-14 code [16] adopted the following expressions to estimate f_{ub} in (MPa). Mainly, when $l/h \leq 35$

$$f_{ub} = f_{pe} + 70 + \frac{f_c'}{100\,\rho_{ps}} \qquad (1)$$
$$f_{ub} \leq the\ least\ of\ (f_{pe} + 420)\ and\ (f_{py})$$

when $l/h > 35$

$$f_{ub} = f_{pe} + 70 + \frac{f_c'}{300\,\rho_{ps}} \qquad (2)$$
$$f_{ub} \leq the\ least\ of\ (f_{pe} + 210)\ and\ (f_{py})$$

where l is the length of the clear span measured face to face of support in mm, h is the overall thickness, height or depth of member in mm, f_{pe} effective stress in prestressing steel after all prestress losses in MPa, $f_c{}'$ is specified compressive strength of concrete in MPa, f_{py} is the specified yield strength of prestressing steel in MPa, and ρ_{ps} is the prestressing steel ratio ($\rho_{ps} = A_{ps}/bd_p$) in which A_{ps} is the area of the prestressed reinforcement in tension zone in mm^2, b is the width of compression flange of the member in mm, and d_p is the distance from the extreme compression fiber to the centroid of prestressing reinforcement in mm.

The objectives of the present study includes the suggestion of a numerical methodology for a nonlinear analysis model to predict the stress in internal unbonded prestressed steel at different stages of exposure of structural concrete members to monotonic static loading and, consequently, to evaluate the strength, deformability, and the load-carrying capacity of such structural members under different types of static loading. Also, verification of the proposed model with the available experimental previous studies will be carried out using test results from Tam and Pannell [17], Du and Tao [18], Harajli and Kanj [19], Campbell and Chouinard [20]. The results of the proposed model will be compared to the results of ACI 318M-14 prediction equations [16].

2. STRAIN COMPONENTS RELATIONSHIP

Non-linear stress-strain relationships ($f_m - \varepsilon_m$) proposed by Karpenko et al. [21] were used for concrete in tension and compression and for steel. These relationships are based on the secant modulus of elasticity of the material $\bar{E}_m$, (see Figs. 1-3), which can be formulated as follow:

$$f_m = \bar{E}_m . \varepsilon_m \tag{3}$$

$$\bar{E}_m = E_m . \nu_m \tag{4}$$

$$\nu_m = \hat{\nu}_m \mp (\nu_o - \hat{\nu}_m)\sqrt{1 - e_{1m}\eta_m - e_{2m}\eta_m^2} \tag{5}$$

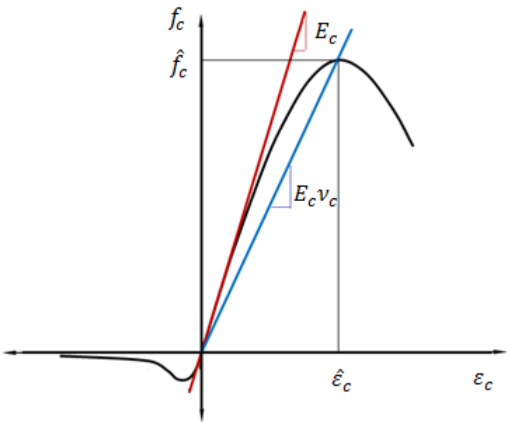

Fig.1 Stress-strain diagram of concrete

where ν_m is the coefficient of elasticity of the material, $\hat{\nu}_m$ is the value of ν_m at the vertex of the stress-strain diagram, ν_o is the value of ν_m at the start of the stress-strain diagram, e_1 and e_2 are diagram curvature parameters in which ($e_{2m} = 1 - e_{1m}$), and η_m is the stress level beyond the proportional limit which can be determined by the following equation:

$$\eta_m = \frac{f_m - f_{m,el}}{\hat{f}_m - f_{m,el}} \quad , \qquad 0 \le \eta_m \le 1 \tag{6}$$

To find the value of ν_m for the material, Eq. (5) can be rearranged in Eq. (7), where the larger root should be considered.

$$\hat{\nu}_m^2 - (\nu_o - \hat{\nu}_m)^2 \left[1 + \frac{e_{1m}\tilde{f}_{m,el}}{1 - \tilde{f}_{m,el}} - \frac{e_{2m}\tilde{f}_{m,el}^{\ 2}}{(1 - \tilde{f}_{m,el})^2}\right] - \nu_m \left[2\hat{\nu}_m - \frac{\tilde{\varepsilon}_m(\nu_o - \hat{\nu}_m)^2}{\hat{\nu}_m(1 - \tilde{f}_{m,el})}\left(e_{1m} - \frac{2e_{2m}\tilde{f}_{m,el}}{1 - \tilde{f}_{m,el}}\right)\right] + \nu_m^2\left[1 + \frac{e_{2m}(\nu_o - \hat{\nu}_m)^2\tilde{\varepsilon}_m^2}{\hat{\nu}_m^2(1 - \tilde{f}_{m,el})^2}\right] = 0 \tag{7}$$

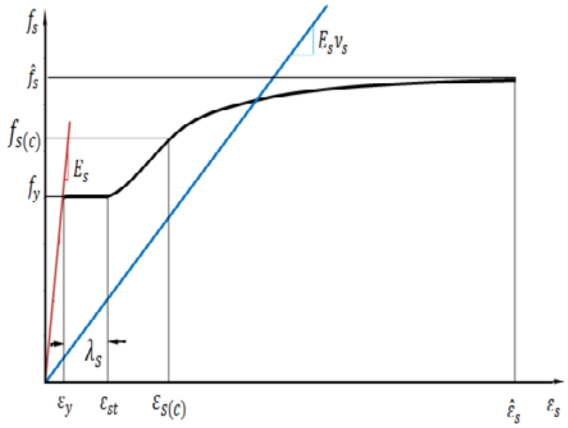

Fig.2 Stress-strain diagram of mild steel

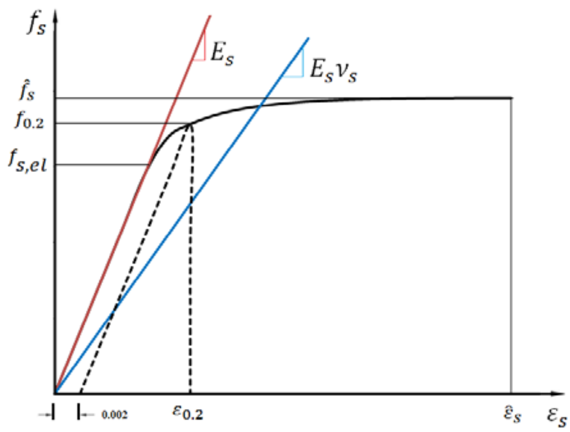

Fig.3 Stress-strain diagram of high strength steel

3. LOAD-STRAIN COMPONENTS RELATIONSHIP

Consider the cross-section of a partially prestressed flexural concrete member that reinforced with internal unbonded post-tensioned steel and ordinary (nonprestressed) mild steel (Fig. 4) and exposed to normal force and biaxial bending moment.

According to the Bernoulli's assumption in which the plane section before bending remains plane after bending, the strain at any fiber can be calculated according to the following expression:

$$\varepsilon_m = (\varepsilon_{mi} + \varepsilon_o) + \psi_x y_m + \psi_y x_m \quad (8)$$

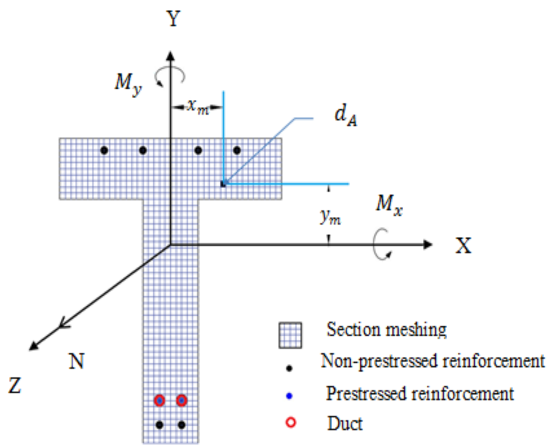

Fig.4 Section geometry and positive sign convention

where ε_{mi} is the initial strain in the material; ε_o is the axial strain at the reference point; ψ_x is the curvature of the member's longitudinal axis in the OYZ plane; ψ_y is the curvature of the member's longitudinal axis in the OXZ plane. Figure (4) shows the adopted positive sign convention.

Equation (8) can be rewritten in a matrix form:

$$\varepsilon_m = Z\,\{\bar{\varepsilon}\} \quad (9)$$

$$Z = \{1 \quad y \quad x\,\} \quad (10)$$

$$\{\bar{\varepsilon}\} = \{(\varepsilon_{mi} + \varepsilon_o) \quad \psi_x \quad \psi_y\,\} \quad (11)$$

While the force vector takes the following shape:

$$\{F\} = \begin{Bmatrix} N \\ M_x \\ M_y \end{Bmatrix} = \begin{Bmatrix} \int_{A_m} f_m \, dA_m \\ \int_{A_m} f_m \, y_m \, dA_m \\ \int_{A_m} f_m \, x_m \, dA_m \end{Bmatrix} \quad (12)$$

Substituting Eq. (3) and Eq. (9), Eq. (12) will adopt a new form

$$\{F\} = \begin{Bmatrix} N \\ M_x \\ M_y \end{Bmatrix} = \begin{bmatrix} C_{11} & C_{12} & C_{13} \\ C_{21} & C_{22} & C_{23} \\ C_{31} & C_{32} & C_{33} \end{bmatrix} \begin{Bmatrix} (\varepsilon_{mi} + \varepsilon_o) \\ \psi_x \\ \psi_y \end{Bmatrix} \quad (13)$$

where C_{ij} is the element (ij) of the stiffness matrix that depends on the geometry of the section and the attained stress-strain condition in the components of the cross-section under the applied load. C_{ij} can be calculated as follow:

$$\begin{aligned} C_{11} &= \bar{E}_m \int_{A_m} dA_m \\ C_{12} = C_{21} &= \bar{E}_m \int_{A_m} y_m \, dA_m \\ C_{13} = C_{31} &= \bar{E}_m \int_{A_m} x_m \, dA_m \\ C_{22} &= \bar{E}_m \int_{A_m} y_m^2 \, dA_m \\ C_{23} = C_{32} &= \bar{E}_m \int_{A_m} y_m \, x_m \, dA_m \\ C_{33} &= \bar{E}_m \int_{A_m} x_m^2 \, dA_m \end{aligned} \quad (14)$$

The stiffness matrix in Eq. (13) depends on the value of $\{\bar{\varepsilon}\}$ which has not determined yet. So an iteration process should be performed in which,

$$\begin{aligned} &\{\bar{\varepsilon}\}_i = [C(\{\bar{\varepsilon}\}_{i-1})]^{-1} * \{F\} \\ &\{\bar{\varepsilon}\}_0 = 0\,, \quad i = 1, 2, 3, \ldots \ldots \end{aligned} \quad (15)$$

Through each iteration the new value of the strain vector $\{\bar{\varepsilon}\}_i$ should be compared to the old value which determined at the previous iteration. The comparison process should be continuing until the convergence is achieved.

Whenever the strain vector is determined, the strain in concrete fibers and in bonded steel reinforcement can be estimated depending on the strain compatibility using Eq. (8). In case of the internal unbonded steel reinforcement, due to the lack of bonding and in turn the violation of the strain compatibility, in this paper, it is suggested that the strain in this type of steel can be calculated by integrating the strain value of concrete at the level of the centroidal axis of the unbonded steel along its entire length and dividing the integrated value by the length of the considered steel between anchorages.

$$\Delta\varepsilon_{ub} = \frac{1}{\ell_{ub}} \int_0^{\ell_{ub}} \Delta\varepsilon_{cub}(z).\,dz \quad (16)$$

where $\Delta\varepsilon_{cub}$ is the change in the strain in the unbonded steel due to the applied load, ℓ_{ub} is the length of the unbonded steel between anchorages, and $\Delta\varepsilon_{cub}$ is the change in strain in concrete fiber at the level of the centroidal axis of the unbonded steel. The value of $\Delta\varepsilon_{ub}$ is considered as the average value for the change of strain along the unbonded steel. Adding $\Delta\varepsilon_{ub}$ to the initial prestrain ε_{ubi} that induced in this steel reinforcement and, consequently, using the constitutive relationship that represents the mentioned steel element, the total stress can be estimated.

$$\varepsilon_{ub} = \varepsilon_{ubi} + \Delta\varepsilon_{ub} \tag{17}$$

$$f_{ub} = f(\varepsilon_{ub}) \tag{18}$$

where f is the nonlinear function that relates the flexural stress in the unbounded steel with its flexural strain.

It is worth to mention that the ultimate flexural stress value is determined when the force vector in Eq. (13) represents the ultimate strength that the critical section can resist.

4. LOAD-DEFLECTION RELATIONSHIP

The deflection value at any point along the beam, during any loading stage, can be determined by distributing the curvature values ψ_x, calculated from Eq. (15) for that loading stage, along the beam and then double integrating them. In this study, Newmark's numerical integration method [22] is utilized to determine deflection values from the curvature using the following procedure (see Fig. 5):

1. The member is divided into an even number of segments by a number of stations or points which are equal to the number of segments plus one. Each point i is with a known value of the curvature $\psi_{x(i)}$ ($\psi_{x(i)}$- fictitious loading on the conjugated beam).
2. The value of equivalent concentrated curvature $\bar{\psi}_{x(i)}$, (fictitious reaction on the conjugated beam), is determined for the left side of the beam using Equations (19) and (20) for the 2nd-degree parabolic curvature (M/EI) and the straight-line curvature, respectively.

$$\bar{\psi}_{x(i)} = \frac{\Delta Z}{12}\left(\psi_{x(i-1)} + 10\psi_{x(i)} + \psi_{x(i+1)}\right) \tag{19}$$

$$\bar{\psi}_{x(i)} = \frac{\Delta Z}{6}\left(\psi_{x(i-1)} + 4\psi_{x(i)} + \psi_{x(i+1)}\right) \tag{20}$$

3. The value of slopes S_i, (fictitious shearing forces in the conjugated beam), which determined sequentially starting from the midspan point C, where:

$$S_c = \frac{\bar{\psi}_{x(c)}}{2} \tag{21}$$

$$S_i = \sum_{j=i}^{c-1} \bar{\psi}_{x(j)} + S_c \tag{22}$$

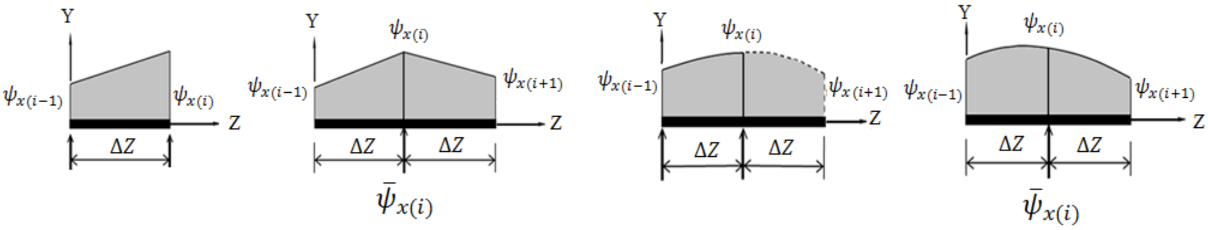

$$\bar{\psi}_{x(i-1,i)} = \frac{\Delta Z}{6}\left(2\,\psi_{x(i-1)} + \psi_{x(i)}\right)$$

$$\bar{\psi}_{x(i,i-1)} = \frac{\Delta Z}{6}\left(\psi_{x(i-1)} + 2\psi_{x(i)}\right)$$

$$\bar{\psi}_{x(i-1,i)} = \frac{\Delta Z}{24}\left(7\,\psi_{x(i-1)} + 6\,\psi_{x(i)}\right) - \psi_{x(i+1)}\Big)$$

$$\bar{\psi}_{x(i,i-1)} = \frac{\Delta Z}{24}\left(3\,\psi_{x(i-1)} + 10\,\psi_{x(i)} - \psi_{x(i+1)}\right)$$

Fig.5 Formulas for equivalent concentrated loads

For a simply supported beam, the values of $\psi_{x(i)}$ and the slope in both ends are unknown; therefore these values can be substituted equal to zero (i.e., $\bar{\psi}_{x(1)}$= 0 and S_c= 0).

4. The value of deflection, (moment in the conjugated beam), for each point, is then determined from Eq. (23).

$$\Delta_i = \sum_{j=2}^{i} S_j\,\Delta_x \tag{23}$$

where $i = 2, 3, \dots\dots, C$.

Since the beam is considered symmetric about midspan, the values of deflection for another half of the beam is determined according to the fact that ($\Delta_{p+1} = \Delta_{n-p}$), where ($p = 1, 2, \dots\dots, C-1$) and n is the number of points (sections) along the beam.

5. VERIFICATION OF LOAD-STRAIN COMPONENTS RELATIONSHIP

To verify and evaluate the proposed methodology for predicting the stress in unbonded steel and in turn the load-carrying capacity of the structural concrete member, experimental data for 60 flexural members with different effective parameters that influenced the above-mentioned stress and strength were collected from other researchers, treated in the present study, and comparisons have been made.

Tam and Pannell [17] tested eight simply supported beams with straight unbonded prestressed reinforcement. The ratio of the clear span of the member l to the effective depth of the prestressed steel d_p was ranged between 18 and 43. These beams were exposed to a single concentrated load at midspan. The experimental and numerical results obtained with the proposed methodology are shown in Table (1).

Du and Tao [18] tested 20 simply supported beams with straight unbonded steel. All beams were with the rectangular cross-sectional configuration of (160 x 280) mm. The span-to-depth ratio of all beams was 19.1, see Table (2).

Table 1 Experimental and numerical results for Tam and Pannell tests [17]

Beam ID	$\frac{l}{d_p}$	Stress at ultimate in unbonded steel f_{ub}, MPa					Failure moment M_u, kN.m				
		test record	proposed methodology		ACI 318M-14 approach		test record	proposed methodology		ACI 318M-14 approach	
		f_{ub}^{exp}	f_{ub}^{est}	$\frac{f_{ub}^{est}}{f_{ub}^{exp}}$	f_{ub}^{est}	$\frac{f_{ub}^{est}}{f_{ub}^{exp}}$	M_u^{exp}	M_u^{est}	$\frac{M_u^{est}}{M_u^{exp}}$	M_u^{est}	$\frac{M_u^{est}}{M_u^{exp}}$
B1	18.0	962.19	914.74	0.951	944.08	0.981	40.13	39.92	0.995	42.75	1.065
B2	23.5	898.43	857.36	0.954	877.01	0.976	60.65	55.68	0.918	69.91	1.153
B3	27.5	1046.40	993.13	0.949	1036.38	0.990	30.75	35.00	1.138	35.96	1.169
B4	28.6	969.68	963.9	0.994	984.20	1.015	38.38	40.24	1.048	47.94	1.249
B5	29.3	1071.84	1079.08	1.007	1097.42	1.024	22.14	25.57	1.155	29.46	1.331
B6	31.4	944.74	964.39	1.021	983.07	1.041	22.47	27.54	1.226	36.07	1.605
B7	38.8	859.97	884.34	1.028	902.43	1.049	22.84	25.67	1.124	31.97	1.400
B8	43.0	732.67	772.5	1.054	833.02	1.137	21.01	18.59	0.885	16.21	0.772
Average of $(f_{ub}^{est}/f_{ub}^{exp})$ or (M_u^{est}/M_u^{exp})				0.995		1.027			1.061		1.218
Standard of deviation (σ)				0.040		0.052			0.121		0.247
Coefficient of variation (COV)				0.040		0.051			0.114		0.203

Table 2 Experimental and numerical results for Du and Tao tests [18]

Beam ID	$\frac{l}{d_p}$	Stress at ultimate in unbonded steel f_{ub}, MPa					Failure moment M_u, kN.m				
		test record	proposed methodology		ACI 318M-14 approach		test record	proposed methodology		ACI 318M-14 approach	
		f_{ub}^{exp}	f_{ub}^{est}	$\frac{f_{ub}^{est}}{f_{ub}^{exp}}$	f_{ub}^{est}	$\frac{f_{ub}^{est}}{f_{ub}^{exp}}$	M_u^{exp}	M_u^{est}	$\frac{M_u^{est}}{M_u^{exp}}$	M_u^{est}	$\frac{M_u^{est}}{M_u^{exp}}$
A1	19.1	1458	1500	1.029	1213	0.832	31.1	30.1	0.968	24.6	0.791
A2	19.1	1430	1362	0.952	1084	0.758	46.8	41.3	0.882	36.6	0.782
A3	19.1	1176	1242	1.056	959	0.815	63.6	54.3	0.854	50.8	0.799
A4	19.1	1465	1447	0.988	1122	0.766	38.3	34.1	0.890	29.3	0.765
A5	19.1	1315	1303	0.991	1017	0.773	51.2	46.8	0.914	43.4	0.848
A6	19.1	1063	1142	1.074	993	0.934	72.4	67.9	0.938	66.5	0.919
A7	19.1	1436	1329	0.925	1230	0.857	41.5	39.9	0.961	37.9	0.913
A8	19.1	1290	1325	1.027	1162	0.901	59.4	56.2	0.946	54.1	0.911
A9	19.1	1108	1099	0.992	1064	0.960	102	90.3	0.886	90.0	0.882
B1	19.1	1645	1679	1.021	1352	0.822	30.3	33.5	1.106	26.8	0.884
B2	19.1	1564	1595	1.020	1221	0.781	50.4	47.3	0.938	40.4	0.802
B3	19.1	1361	1443	1.060	1128	0.829	61.0	62.8	1.030	57.6	0.944
B5	19.1	1520	1538	1.012	1250	0.822	53.4	52.5	0.983	48.1	0.901
B6	19.1	1402	1409	1.005	1181	0.842	75.8	74.3	0.980	71.4	0.942
B7	19.1	1603	1583	0.988	1422	0.887	42.5	43.9	1.033	40.7	0.958
B9	19.1	1346	1402	1.042	1295	0.962	89.7	93.5	1.042	92.4	1.030
C1	19.1	1396	1423	1.019	1173	0.840	33.6	35.9	1.068	28.6	0.851
C3	19.1	1316	1249	0.950	969	0.736	67.3	59.5	0.884	54.2	0.805
C7	19.1	1411	1398	0.991	1322	0.937	44.6	50.5	1.132	44.3	0.993
C9	19.1	1109	1096	0.988	1047	0.944	101.0	98.0	0.970	101.6	1.006
Average of $(f_{ub}^{est}/f_{ub}^{exp})$ or (M_u^{est}/M_u^{exp})				1.007		0.850			0.970		0.886
Standard of deviation (σ)				0.038		0.071			0.078		0.079
Coefficient of variation (COV)				0.038		0.084			0.080		0.089

The main variables were the area of prestressed steel A_{ps}, the concrete compressive strength $f_c{}'$, and the effects of varying amounts of nonprestressed reinforcement A_s on the stress in unbonded prestressed tendons in partially prestressed concrete beams at ultimate load. All tested specimens were exposed to a progressively increased, up to the failure, third point monotonic static loading over (4200) mm effective span. Table (2) shows the experimental and the calculated, according to the proposed methodology and the ACI 318M-14 approach results for the ultimate stress in unbonded prestressed steel and the failure moments.

Harajli and Kanj [19] tested 26 simply supported partially prestressed concrete beams with three groups having span-to-depth ratios equal to 19, 12 and 7.8, respectively. Three different contents of tension reinforcement (i.e., reinforcing index) were used. In their experimental program, thirteen beams were subjected to a single concentrated static loading at the midspan section, while the other 13 specimens were exposed to third-point static loading. All beams were tested up to failure. The comparison of the experimental and the numerical results for the ultimate stress in unbonded prestressed steel and the failure moments are shown in Table (3).

Campbell and Chouinard [20] tested six simply supported partially presressed concrete beams of a rectangular cross-section of (160 x 220) mm dimensions and (3300) mm span length. All beams were subjected to third-point monotonic static loading. The span-to-depth ratio was 15 for all beams. The main variable was the effect of the amount of bonded nonprestressed reinforcement on the stress in unbonded prestressing steel. Table (4) shows the comparison of the experimental and numerical outcomes. Tables (2)-(4) show also the average values of the estimated to the experimental results at failure, the standard of deviation, and the coefficient of variation. Figures 6 to 9 illustrate the scattering of the numerical results of the proposed methodology from the experimental findings.

Table 3 Experimental and numerical results for Harajli and Kanj tests [19]

Beam ID	$\frac{l}{d_p}$	Stress at ultimate in unbonded steel f_{ub}, MPa					Failure moment M_u, kN.m	
		test record	proposed methodology		ACI 318M-14 approach		proposed methodology	ACI 318M-14 approach
		f_{ub}^{exp}	f_{ub}^{est}	$\frac{f_{ub}^{est}}{f_{ub}^{exp}}$	f_{ub}^{est}	$\frac{f_{ub}^{est}}{f_{ub}^{exp}}$	M_u^{est}	M_u^{est}
PP2R3-3	19.0	1261.3	1284.6	1.018	1247.7	0.989	21.2	17.9
PP2R3-0	19.0	1245.6	1178.4	0.946	1238.0	0.994	19.3	15.6
PP3R3-3	19.0	1106.9	1155.7	1.044	1066.1	0.963	32.7	30.2
PP3R3-0	19.0	1068.9	1002.1	0.938	1068.9	1.000	32.7	32.5
P1R3-3	19.0	1280.0	1348.7	1.054	1365.8	1.067	14.0	7.0
P1R3-0	19.0	1351.7	1351.1	1.000	1366.1	1.011	14.4	7.0
P2R3-3	19.0	1212.4	1262.0	1.041	1055.0	0.870	20.3	15.2
P2R3-0	19.0	1206.9	1147.9	0.951	1046.9	0.867	19.6	15.0
P3R3-3	19.0	1160.7	1178.1	1.015	1033.8	0.891	25.5	20.5
P3R3-0	19.0	1127.6	1107.6	0.982	990.3	0.878	24.4	19.7
PP1R2-3	12.0	1281.3	1231.0	0.961	1224.0	0.955	33.21	30.9
PP1R2-0	12.0	1229.7	1218.7	0.991	1187.6	0.966	33.6	29.7
PP2R2-3	12.0	1217.2	1227.5	1.009	1098.8	0.903	41.8	37.9
PP2R2-0	12.0	1259.3	1154.6	0.917	1077.9	0.856	41.2	37.6
PP3R2-3	12.0	1086.2	1160.5	1.068	1057.7	0.974	63.1	61.2
PP3R2-0	12.0	1157.2	1124.9	0.972	1089.2	0.941	63.75	61.7
P1R2-3	12.0	1400.0	1415.2	1.011	1231.5	0.880	24.1	18.1
P1R2-0	12.0	1205.5	1210.7	1.004	1036.8	0.860	26.8	19.8
P2R2-3	12.0	1233.1	1234.8	1.001	1014.4	0.823	34.3	27.0
P2R2-0	12.0	1186.2	1169.9	0.986	1009.5	0.851	34.4	26.9
PP1R1-3	7.8	1200.0	1240.4	1.034	1185.8	0.988	49.2	42.7
PP1R1-0	7.8	1281.3	1155.4	0.901	1213.0	0.947	49.9	44.5
PP2R1-3	7.8	1217.2	1203.0	0.988	1140.9	0.937	75.1	68.0
PP2R1-0	7.8	1182.8	1161.9	0.982	1103.6	0.933	65.0	56.7
PP3R1-3	7.8	1120.7	1169.5	1.044	1053.2	0.940	79.7	71.0
PP3R1-0	7.8	1079.3	1102.9	1.022	1043.3	0.967	79.6	70.7
Average of $(f_{ub}^{est}/f_{ub}^{exp})$				0.995		0.933		
Standard of deviation (σ)				0.042		0.060		
Coefficient of variation (COV)				0.042		0.064		

Table 4 Experimental and numerical results for Campbell and Chouinard tests [20]

Beam ID	$\frac{l}{d_p}$	Stress at ultimate in unbonded steel f_{ub}, MPa: test record f_{ub}^{exp}	proposed methodology f_{ub}^{est}	proposed methodology $\frac{f_{ub}^{est}}{f_{ub}^{exp}}$	ACI 318M-14 approach f_{ub}^{est}	ACI 318M-14 approach $\frac{f_{ub}^{est}}{f_{ub}^{exp}}$	Failure moment M_u, kN.m: test record M_u^{exp}	proposed methodology M_u^{est}	proposed methodology $\frac{M_u^{est}}{M_u^{exp}}$	ACI 318M-14 approach M_u^{est}	ACI 318M-14 approach $\frac{M_u^{est}}{M_u^{exp}}$
1	15	1476	1420	0.962	1228	0.832	45.5	42.3	0.930	48.5	0.801
2	15	1467	1411	0.962	1212	0.826	63.3	55.7	0.880	63.5	0.832
3	15	1381	1320	0.956	1194	0.865	81.1	68.4	0.843	76.5	0.828
4	15	1348	1332	0.988	1254	0.930	98.0	85.4	0.871	92.7	0.866
5	15	1274	1263	0.991	1240	0.973	105.5	97.8	0.927	103.5	0.929
6	15	1269	1223	0.964	1245	0.980	120.2	109.4	0.910	113.2	0.916
Average of ($f_{ub}^{est}/f_{ub}^{exp}$) or ($M_u^{est}/M_u^{exp}$)				0.970		0.901			0.894		0.980
Standard of deviation (σ)				0.015		0.070			0.034		0.049
Coefficient of variation (COV)				0.016		0.077			0.038		0.050

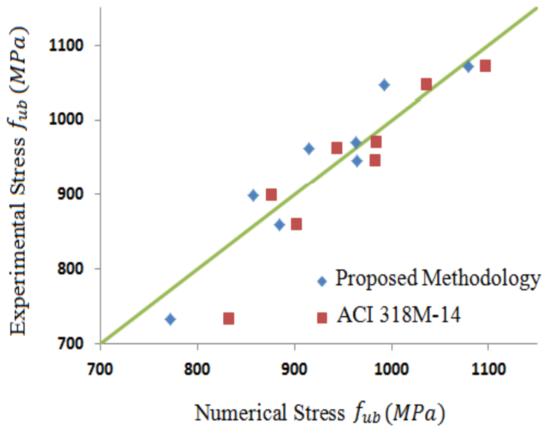

Fig. 6 Experimental and numerical stress relationship at ultimate in unbonded steel for Tam and Pannell tests [17]

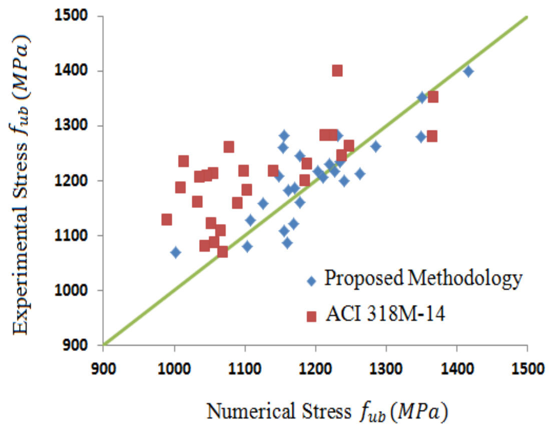

Fig. 8 Experimental and numerical stress relationship at ultimate in unbonded steel for Harajli and Kanj tests [19]

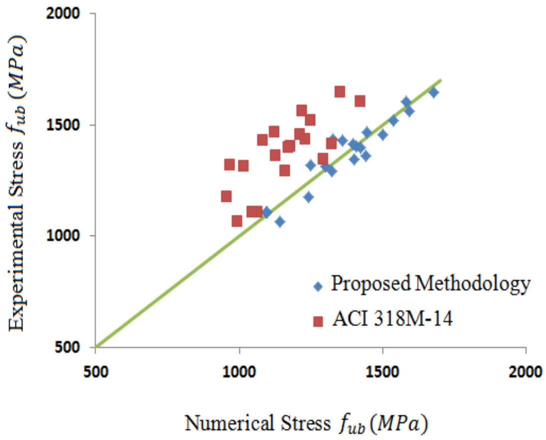

Fig. 7 Experimental and numerical stress relationship at ultimate in unbonded steel for Du and Tao tests [18]

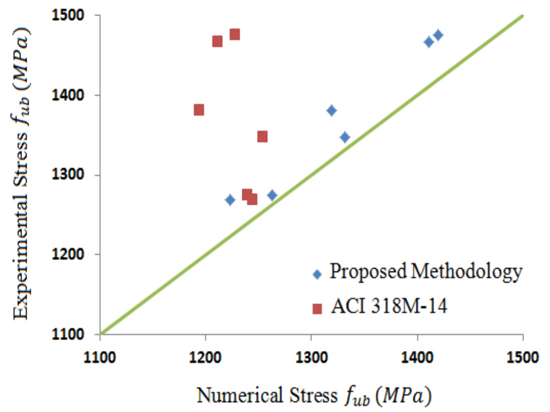

Fig. 9 Experimental and numerical stress relationship at ultimate in unbonded steel for Campbell and Chouinard tests [20]

6. VERIFICATION OF LOAD-DEFLECTION RELATIONSHIP

To verify the predicted values of deflection, experimental data are also used for other researchers. Du and Tao [18] reported the experimental values of midspan deflection for 22 of the tested beams, (even they reported the results of stress in the unbounded tendons for only 20 tested beams). Table (5) shows the comparison between the proposed in this study methodology for computing deflection to the experimental values and to the values obtained theoretically by Du and Tao [18].

Table 5 Experimental and numerical results of midspan deflection values for Du and Tao tests [18]

Beam ID	Deflection at ultimate load (mm)					Beam ID	Deflection at ultimate load (mm)				
	test record	proposed methodology		Du and Tao methodology			test record	proposed methodology		Du and Tao methodology	
	Δ^{exp}	Δ^{est}	$\frac{\Delta^{est}}{\Delta^{exp}}$	$\Delta^{[18]}$	$\frac{\Delta^{[18]}}{\Delta^{exp}}$		Δ^{exp}	Δ^{est}	$\frac{\Delta^{est}}{\Delta^{exp}}$	$\Delta^{[18]}$	$\frac{\Delta^{[18]}}{\Delta^{exp}}$
A1	110.7	107.93	0.975	108.9	0.984	B3	68.5	62.17	0.908	61.8	0.902
A2	100.0	71.45	0.715	71.5	0.715	B4	123.7	108.24	0.875	119.0	0.962
A3	57.3	57.27	0.999	52.0	0.908	B5	99.6	74.06	0.744	81.8	0.821
A4	119.0	96.11	0.808	93.9	0.789	B6	66.6	53.82	0.808	46.8	0.703
A5	75.4	65.49	0.869	64.7	0.858	B7	103.0	81.975	0.796	120.1	1.166
A6	44.5	45.2	1.016	43.2	0.971	B8	99.8	68.58	0.687	74.3	0.744
A7	101.5	87.26	0.86	79.6	0.784	B9	48.5	46.55	0.96	54.2	1.118
A8	70.9	57.5	0.811	60.9	0.859	C1	81.8	82.91	1.014	104.2	1.274
A9	39.4	35.37	0.898	37.2	0.944	C3	65.4	57.97	0.886	52.9	0.809
B1	109.2	115.26	1.055	138.2	1.266	C7	73.0	73.33	1.004	82.0	1.123
B2	92.5	88.15	0.953	93.8	1.014	C9	43.4	39.63	0.913	36.2	0.834
Average of ($\frac{\Delta^{est}}{\Delta^{exp}}$) or ($\frac{\Delta^{[18]}}{\Delta^{exp}}$)									0.889		0.934
Standard of deviation (σ)									0.103		0.168
Coefficient of variation (COV)									0.116		0.180

7. CONCLUSIONS

The methodology presented in this paper focuses on the determination of the stress in unbonded prestressing steel and bonded conventional reinforcement, the curvature and the deflection of the section at different loading stages including the nominal strength, in addition to, the load-carrying capacity of the structural concrete members under different effects of static loading.

Based on the results of the numerical investigation, the following conclusions are drawn:

1. The comparison of the numerical results of the stress in unbonded prestressing steel at ultimate determined according to the proposed in this paper methodology to the experimental data of 60 structural concrete members tested between 1976 and 1991 showed that the average value of the estimated to the experimental stresses at failure is 0.997 with a standard of deviation and coefficient of variation each of 0.039. On the other hand, these values attained 0.914, 0.085, 0.093, respectively, according to the analytical method-ology proposed by the ACI 318M-14.
2. The comparison of the numerical results of the proposed methodology of the failure moment to the test data available for 34 structural concrete members proved that the average value of the predicted to the observed during testing failure moments is 0.978 with a standard of deviation and coefficient of variation of 0.099 and 0.101, respectively. Meanwhile, these values reached 0.96, 0.195, 0.203, respectively, based on the ACI 318M-14 approach.
3. The comparison of the numerical midspan deflection to the available experimental findings for 22 structural concrete members indicated that the average value for the estimated to the measured deflections is 0.889 with a standard of deviation and coefficient of variation of 0.103, and 0.116, respectively.

8. REFERENCES

[1] Warwaruk J., Sozen M.A., and Siess C.P., Investigation of Prestressed Reinforced Concrete for Highway Bridge, Part III: Strength and Behavior in Flexure of Prestressed Concrete Beams, University of Illinois Engineering Experiment Station Bulletin No. 464, Urban, III, August 1962, pp. 1-105.

[2] Pannell F. N." The Ultimate Moment of Resistance of Unbonded Prestressed Concrete Beams" Magazine of Concrete Research: Vol. 21, No. 66, March 1969, pp. 43-54.

[3] Mattock A. H., Yamazaki J. and Kattula B.T., Comparative Study of Prestressed Concrete

Beams, With and Without Bond, ACI Journal, Vol. 68, No. 3, Feb. 1971, pp. 116-125.

[4] Mojtahedi S. and Gamble W. L., Ultimate Steel Stresses in Unbonded Prestressed Concrete, ASCE, Vol. 104, No. ST7, July 1978, pp. 1159-1165.

[5] Diep B. K. and Niwa J., Prediction of Loading-Induced Stress in Unbonded Tendons at Ultimate, Doboku Gakkai Ronbunshuu E, Vol. 62, No. 2. 2006, pp. 428-443.

[6] Ozkul O., Nassif H., Tanchan P., and Harajli, M., Rational Approach for Predicting Stress in Beams with Unbonded Tendons, ACI Structural Journal, 105 (3). 2008, pp. 338-347.

[7] Harajli M., Tendon Stress at Ultimate in Continuous Unbonded Post-Tensioned Members: Proposed Modification of ACI 318, Eq. (18-4) and (18-5), ACI Structural Journal, Vol. 109, No. 2, March-April. 2012, pp. 183-192.

[8] Su J., Yi N., Sun Z., Bai Y. and Zhang A., Experimental Study on Mechanical Performance of Unbonded and Bonded Prestressed Concrete Beams, Applied Mechanics and Materials Vol. 178-181.2012, pp. 2387-2392.

[9] El Meski F. and Harajli M., Flexural Behavior of Unbonded Posttensioned Concrete Members Strengthened Using External FRP Composites, Journal of Composites for Construction, March-April, 2013, pp.197-207.

[10] Heo S., Shin S. and Lee C., Flexural Behavior of Concrete Beams Internally Prestressed with Unbonded Carbon-Fiber-Reinforced Polymer Tendons, Journal of Composites for Construction, Vol. 17, No. 2, April 1.2013, pp. 167-175.

[11] Maguire A., Collins W. N., Halbe, K. R. and Roberts-Wollmann, C. L., Multi-Span Members with Unbonded Tendons: Ultimate Strength Behavior, ACI Structural Journal, Vol. 113, No. 2, March-April. 2016, pp.195-204.

[12] Maghsoudi M. and Maghsoudi A. A., Experimental and Theoretical Serviceability of Strengthened and Nonstrengthened Unbonded Posttensioned Indeterminate I-Beams, J. Bridge Eng., Vol. 22, No.7, 2017, p. 05017006, pp.1-16.

[13] Six P., Tawadrous R., Syndergaard, P. and Maguire M., Flexural Behavior of Three Span Continuous Unbonded Post-tensioned Members with Variable Bonded Reinforcement, Engineering Structures, 200 (2019) 109704, pp. 1-12.

[14] Khattab M. M. and Oukaili N. K., Partially Prestressed Concrete Beams Under Limited Cycles of Repeated Loading, Journal of Engineering Science and Technology, Vol. 14, No. 2, April 2019, pp.965-986.

[15] Xue W. and Peng F., Calculating Method for Ultimate Tendon Stress in Internally Unbonded Prestressed Concrete Members, ACI Structural Journal, Vol.116, No. 5, September 2019, pp. 225-233.

[16] ACI Committee 318, Building Code Requirement for Reinforced Concrete (ACI 318-2014), American Concrete Institute, 2014, pp.1-506.

[17] Tam A. and Pannell F. N., The Ultimate Moment of Resistance of Unbounded Partially Prestressed Reinforced Concrete Beams, Magazine of Concrete Research, Vol. 28, No. 97 December 1976, pp. 203-208.

[18] Du G. and X. Tao, Ultimate Stress in Unbonded Tendons of Partially Prestressed Concrete Beams, PCI Journal, Vol. 30, No. 6, November-December, 1985, pp. 72-91.

[19] Harajli M., and Kanj M., Ultimate Flexural Strength of Concrete Members Prestressed with Unbonded Tendons, ACI Structural Journal, Vol. 88, No. 6, Nov.-Dec. 1991, pp. 663-673.

[20] Campbell I.T. and Chouinard K.I., Influence of Non-prestressed Reinforcement on the Strength of Unbounded Partially Prestressed Concrete Members, ACI Structural Journal, Vol.88, No.5, 1991, pp. 546-551.

[21] Karpenko N.I., Mukhamediev T.A. and Petrov A.N. ,The Initial and Transformed Stress-strain Diagrams of Steel and Concrete, Special Publication, Stress-Strain Condition for Reinforced Concrete Construction, Reinforced Concrete Research Center, Moscow, 1986, pp. 7-25.

[22] Newmark N. M., Numerical Procedure for Computing Deflections, Moments and Buckling Loads, Transactions, ASCE,108, 1943, pp. 1161-1234.